Scheibe, Benjamin; Haiges, Ralf; Ivlev, Sergei I.; Karttunen, Antti J.; Müller, Ulrich; Christe, Karl O.; Kraus, Florian

Difluorochloronium(III) Fluoridometallates - from Molecular Building Blocks to (Helical) Chains

Published in:
European Journal of Inorganic Chemistry

DOI:
10.1002/ejic.202000845

Published: 20/12/2020

Document Version
Publisher's PDF, also known as Version of record

Please cite the original version:
Scheibe, B., Haiges, R., Ivlev, S. I., Karttunen, A. J., Müller, U., Christe, K. O., & Kraus, F. (2020). Difluorochloronium(III) Fluoridometallates - from Molecular Building Blocks to (Helical) Chains. *European Journal of Inorganic Chemistry*, *2020*(47), 4483-4496. https://doi.org/10.1002/ejic.202000845

EurJIC
European Journal of Inorganic Chemistry

Full Paper
doi.org/10.1002/ejic.202000845

Chemi
Europ
European C
Societies P

Halogen Bonding

Difluorochloronium(III) Fluoridometallates – from Molecular Building Blocks to (Helical) Chains

Benjamin Scheibe,[a] Ralf Haiges,[b] Sergei I. Ivlev,[a] Antti J. Karttunen,[c] Ulrich Müller,[a] Karl O. Christe,[b] and Florian Kraus*[a]

Abstract: Difluorochloronium(III) compounds were synthesized from the reaction of metal powders (Ru, Os, Ir, Au), metal fluorides (NbF_5, SbF_3, BiF_5) or a metal chloride ($TaCl_5$) with excess liquid chlorine trifluoride. The compounds $ClF_2[AuF_4]$, $ClF_2[MF_6]$ (M = Nb, Ta, Ru, Os, Ir, Sb, Bi) and $ClF_2[Ta_2F_{11}]$ were obtained in crystalline form and their crystal structures were determined by single-crystal X-ray diffraction. The ClF_2^+ cations in the investigated compounds are bent, containing two strong, short, mainly covalent Cl–F bonds and two sterically active, free valence electron pairs in a pseudo-tetrahedral arrangement. The coordination around the Cl atom is extended by two highly ionic, long fluorine bridges to neighboring fluoridometallate anions, resulting in a total coordination number of six. The crystal structures vary among the ClF_2^+ compounds and range from molecular building blocks, such as dimeric $(ClF_2[AuF_4])_2$ and $(ClF_2[Ta_2F_{11}])_2$, to chains, some of which being helical, as in $ClF_2[MF_6]$, (M = Nb, Ta, Ru, Os, Ir, Sb, Bi). Quantum-chemical solid-state and gas-phase calculations were carried out to elucidate the bonding within the ClF_2^+ cations and their interactions with the bridging F atoms.

Introduction

Chlorine trifluoride is one of the most reactive compounds and reacts vigorously with many metals, metal oxides and especially with most organic compounds, if the reaction conditions are not well controlled.[1–4] The reactivity of ClF_3 at ambient temperature surpasses that of elemental fluorine. The products from reactions of ClF_3 with metals, such as Mo, W, U, and metal oxides, such as UO_2, ReO_3, OsO_4, are usually fluorides (MF_6, M = Mo, W, U) and oxyfluorides ($ReOF_5$, OsO_3F_2), respectively, in high or highest oxidation states.[5–8]

If ClF_3 is used in excess and reacted with a fluoride that has an appreciable fluoride ion affinity, such as AsF_5 or SbF_5, a difluorochloronium(III) compound is formed.[9,10] With weaker Lewis acids, such as BF_3 and PF_5, thermally unstable ClF_2^+ salts, are formed.[11] This amphoteric character is common for all halogen trifluorides, XF_3 (X = Cl, Br, I). They can form bent, C_{2v}-symmetric XF_2^+ cations and square planar D_{4h}-symmetric $[XF_4]^-$ anions, see Equation (1) and Equation (2) and Scheme 1.[9,10,12–20]

$$XF_3 + MF_5 \longrightarrow XF_2[MF_6] \tag{1}$$

X = Cl, Br, I; M = As, Sb

$$XF_3 + AF \longrightarrow A[XF_4] \tag{2}$$

X = Cl, Br, I; A = K, Rb, Cs

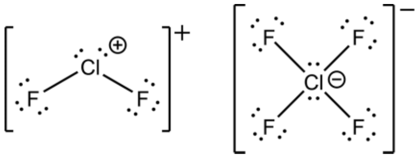

Scheme 1. Lewis structures of the ClF_2^+ cation and the ClF_4^- anion.

Fluorohalonium(III) cations with higher nuclearity have recently been reported for the BrF_3 system: $[Br_2F_5]^+$ and $[Br_3F_8]^+$ are formed according to Equation (3).[21] In these cations, μ_2-bridging fluorine atoms are present, but so far no evidence for such type of cations has been reported for ClF_3 and IF_3.

$$BrF_2[SbF_6] + n\,BrF_3 \longrightarrow [Br_{1+n}F_{2+3n}][SbF_6] \tag{3}$$

n = 1, 2

Several ClF_2^+ salts have previously been structurally characterized by single-crystal X-ray diffraction. Crystal structures were reported for $ClF_2[BF_4]$ and $ClF_2[MF_6]$ (M = Nb, Ta, Ru, Os, As, Sb, Bi).[9,10,22–26] In the reported crystal structure of $ClF_2[OsF_6]$, a disordered ClF_2^+ cation was proposed, which prompted us to redetermine some of the reported crystal structures.

---

[a] B. Scheibe, Dr. S. I. Ivlev, Prof. em. Dr. U. Müller, Prof. Dr. F. Kraus
Fachbereich Chemie, Philipps-Universität Marburg,
Hans-Meerwein-Straße 4
35032 Marburg, Germany
E-mail: f.kraus@uni-marburg.de
https://www.uni-marburg.de/en/fb15/researchgroups/ag-kraus
[b] Prof. Dr. R. Haiges, Prof. Dr. K. O. Christe
Department of Chemistry, University of Southern California,
Los Angeles, CA 90089, USA
[c] Prof. Dr. A. J. Karttunen
Department of Chemistry and Materials Science, Aalto University,
00076 Aalto, Finland

Supporting information and ORCID(s) from the author(s) for this article are available on the WWW under https://doi.org/10.1002/ejic.202000845.

Here, we report on the syntheses of several $\mathrm{ClF_2^+}$ compounds ($\mathrm{ClF_2}[M\mathrm{F_6}]$, M = Nb, Ta, Ru, Os, Ir, Sb, Bi; $\mathrm{ClF_2[Ta_2F_{11}]}$; $\mathrm{ClF_2[AuF_4]}$) and the determination of their crystal structures by single-crystal X-ray diffraction. Some of the crystal structures were redetermined with higher precision than before to see if the reported space groups or structural models were correct. For example, the previously reported crystal structure of $\mathrm{ClF_2[OsF_6]}$ with a disordered $\mathrm{ClF_2^+}$ cation seemed questionable. Furthermore, quantum-chemical calculations are presented for the solid-state crystal structures as well as for the corresponding free gas-phase fragments, $[\mathrm{ClF_2}[M\mathrm{F_6}]_2]^-$ (M = Nb, Ta, Ru, Os, Ir, As, Sb, Bi), $[\mathrm{ClF_2(HF)_2}]^+$, $(\mathrm{ClF_2[Ta_2F_{11}]})_2$, $(\mathrm{ClF_2[AuF_4]})_2$, and $(\mathrm{ClF_2[BF_4]})_2$, to elucidate the chemical bonding. The $\mathrm{ClF_2^+}$ containing compounds reported here are enormously powerful oxidizers. One of the authors (KOC) has demonstrated in classified unpublished work at Rocketdyne the potential of $\mathrm{ClF_2^+}$ salts as an incendiary for Diesel fuel.

Results and Discussion

Synthesis of Difluorochloronium(III) Compounds

Difluorochloronium(III) compounds were synthesized by either reacting metal powders (Ru, Os, Ir, Au), (**Caution!** ***The reactions of metal powders with $\mathrm{ClF_3}$ are highly exothermic and can result in explosions when scaled up)***, metal fluorides ($\mathrm{NbF_5}$, $\mathrm{BiF_5}$, $\mathrm{SbF_3}$) or a chloride ($\mathrm{TaCl_5}$) with an excess of liquid chlorine trifluoride. The reactions can be described by the following idealized Equation (3) to (8). The compounds were isolated in crystalline form from the respective solutions or suspensions by slow removal of excess $\mathrm{ClF_3}$ in vacuo. The crystal structures were subsequently determined by single-crystal X-ray diffraction.

Reactions of Metals with $\mathrm{ClF_3}$

The transition metals Ru, Os and Ir react with $\mathrm{ClF_3}$ at room temperature and are oxidized to the +V oxidation state, giving $\mathrm{ClF_2}[M\mathrm{F_6}]$ (Equation 4).

$$2\,M + 7\,\mathrm{ClF_3} \longrightarrow 2\,\mathrm{ClF_2}[M\mathrm{F_6}] + 5\,\mathrm{ClF} \qquad (4)$$

M = Ru, Os, Ir

Gold also reacts with $\mathrm{ClF_3}$ at room temperature and is oxidized to the +III oxidation state, yielding $\mathrm{ClF_2[AuF_4]}$ (Equation 5).

$$2\,\mathrm{Au} + 5\,\mathrm{ClF_3} \longrightarrow 2\,\mathrm{ClF_2[AuF_4]} + 3\,\mathrm{ClF} \qquad (5)$$

Reactions of Fluorides with $\mathrm{ClF_3}$

The reactions of the fluorides $\mathrm{NbF_5}$ and $\mathrm{BiF_5}$ with $\mathrm{ClF_3}$ lead directly to the formation of the $\mathrm{ClF_2}[M\mathrm{F_6}]$ compounds (Equation 6). When $\mathrm{SbF_3}$ is reacted with $\mathrm{ClF_3}$, $\mathrm{ClF_2[SbF_6]}$ is formed in a vigorous and strongly exothermic reaction (Equation 7).

$$M\mathrm{F_5} + \mathrm{ClF_3} \longrightarrow \mathrm{ClF_2}[M\mathrm{F_6}] \qquad (6)$$

M = Nb, Bi

$$\mathrm{SbF_3} + 2\,\mathrm{ClF_3} \longrightarrow \mathrm{ClF_2[SbF_6]} + \mathrm{ClF} \qquad (7)$$

Reactions of Chlorides with $\mathrm{ClF_3}$

From the reaction of $\mathrm{TaCl_5}$ with $\mathrm{ClF_3}$ both $\mathrm{ClF_2[TaF_6]}$ and $\mathrm{ClF_2[Ta_2F_{11}]}$ could be obtained (Equation 8 and Equation 9).

$$\mathrm{TaCl_5} + 6\,\mathrm{ClF_3} \longrightarrow \mathrm{ClF_2[TaF_6]} + 10\,\mathrm{ClF} \qquad (8)$$

$$2\,\mathrm{TaCl_5} + 11\,\mathrm{ClF_3} \longrightarrow \mathrm{ClF_2[Ta_2F_{11}]} + 20\,\mathrm{ClF} \qquad (9)$$

Idealized equations are given for all the reactions as for simplicity the exclusive formation of ClF was assumed. The formation of $\mathrm{Cl_2}$ is also possible, as ClF can also act as an oxidizer and fluorinating agent.[27] Any formed $\mathrm{Cl_2}$ might react with excess $\mathrm{ClF_3}$ to give ClF, although the reaction is slow, even at elevated temperature and pressure.[28–30]

A Short Introduction to the Symmetry of Polymeric Chainlike Molecules

In all the studied difluorochloronium(III) compounds, the $\mathrm{ClF_2^+}$ cations are associated with the anions resulting in dimeric or polymeric molecules. For the crystallographer these would be one-dimensional infinite strands, however, for reasons that will become clear below, we will use here terms common in polymer chemistry. Some of the polymeric molecules adopt helical configurations. That means there is a *polymer main chain* consisting of atoms held together by a continuous sequence of covalent bonds or similar atomic contacts. The atoms of the main chain are situated on imagined interleaving spirals, one spiral for each kind of atoms. Each spiral is a continuous line that winds at a constant distance around a straight line, the *spiral axis*. The helix consists of *chemically* equivalent *repeating units*. In polymer chemistry, according to the *equivalence postulate*, it is assumed that the repeating units can be treated as if they were symmetry equivalent, even if this is only approximately true.[31,32]

The chemical configuration of a helical molecule is specified as an *N*/*r* helix. *N* is the number of repeating units per translation period, and *r* is the number of the corresponding coil turns (360° turns). *N* and *r* are positive integers without a common divisor. An additional letter *P* or *M* indicates whether the spiral is right- or left-handed.

The term *molecular symmetry* usually refers to the symmetry of an isolated non-polymeric or polymeric molecule, meaning that the influence of any surroundings of the molecule is neglected. The molecular symmetry of a chainlike polymeric molecule that has translational symmetry in only one unique direction is designated by a *rod group*.[33] It is specified in the same way as a space group by its Hermann-Mauguin symbol, but beginning with a script style $\mathcal{p}$ and referring to *c* as the unique direction. Crystallographic rod groups have been compiled in the *International Tables for Crystallography*, Volume E.[33] They contain rotation or screw axes of the orders 1, 2, 3, 4, and 6. However, in a rod group the order of a symmetry axis that points in the unique direction is not restricted to these numbers. Being defined differently, the handedness of the chemical helix and of the corresponding screw axis can be opposite; for example, a chemically left-handed 3/2*M* helix has a right-handed 3_1 screw axis. For more details concerning the symmetry of helical molecules see the literature.[34]

The symmetry of a molecule in a crystal must conform to the crystal symmetry. For a non-polymeric molecule that is the site symmetry (point group) of its Wyckoff position. For a chain-like polymeric molecule it is its rod-site symmetry, called *penetration rod group*.[33] The site symmetry or the penetration rod group is a common subgroup of the space group and of the point group or rod group of the molecular symmetry, respectively.

The Crystal Structures of Difluorochloronium(III) Compounds

The Crystal Structure of $ClF_2[IrF_6]$

Difluorochloronium(III) hexafluoridoiridate(V) crystallizes in the monoclinic space group *P*12/*n*1 (No. 13) with two formula units per unit cell, Pearson code *mP*20 and Wyckoff sequence 13.*g*⁴*fe*. See Table 1 for selected crystallographic data and details of the structure determination. Atomic coordinates, equivalent isotropic and anisotropic displacement parameters are reported in the Supporting Information.

The Cl atom occupies the Wyckoff position 2*f* (site symmetry 2) and is surrounded by the fluorine atoms F(1) and F(1)#1, forming the ClF_2^+ cation, see Figure 1. The Cl–F bond length is 1.573(3) Å and the F(1)–Cl(1)–F(1)#1 angle is 97.1(2)°. The Ir atom occupies the 2*e* position (site symmetry 2) and is surrounded by the fluorine atoms F(2) to F(4) and F(2)#2 to F(4)#2 in the shape of a distorted octahedron. The Ir–F bond lengths are 1.860(3)-1.913(3) Å. For comparison, the Ir–F bond length in $Li[IrF_6]$ is 1.879(5) Å at 299 K.[35] The Ir(1)–F(2) bond length of 1.913(3) Å is significantly longer than the other Ir–F bond lengths, due to a close contact of 2.300(3) Å to the Cl atom. The corresponding F(2)•••Cl(1)•••F(2)#1 angle is 90.38(14)°. The chlorine atom is thus surrounded by four fluorine atoms in a planar-quadrangular fashion (the distance of Cl(1) from the least-squares plane of the surrounding F atoms is 0 Å, due to symmetry).

When these close Ir–F•••Cl contacts are taken into account, a chain along the *a* axis with *trans*-bridging $[IrF_6]^-$ anions results, see Figure 2. The resulting chain has the rod group symmetry

Table 1. Selected crystallographic data and details of the structure determinations of difluorochloronium(III) hexafluoridometallates(V).

	$ClF_2[IrF_6]$	$ClF_2[SbF_6]$	$ClF_2[BiF_6]$	$ClF_2[NbF_6]$	$ClF_2[TaF_6]$
Formula	$ClIrF_8$	$ClSbF_8$	$ClBiF_8$	$ClNbF_8$	$ClTaF_8$
Molar mass/g mol^{-1}	379.66	309.20	455.97	280.35	368.39
Space group (No.)	*P*12/*n*1 (13)	$P\bar{1}$ (2)	$P\bar{1}$ (2)	*Pcca* (54)	*Pcca* (54)
a/Å	6.832(2)	5.1571(5)	5.1564(4)	9.9239(4)	9.9577(6)
b/Å	5.5944(16)	5.5369(5)	5.6670(4)	5.7712(3)	5.7530(3)
c/Å	7.571(2)	10.4111(10)	10.5324(8)	10.4941(4)	10.5389(6)
α/°	90	91.576(8)	91.285(2)	90	90
β/°	94.450(4)	93.507(8)	94.197(2)	90	90
γ/°	90	91.386(7)	92.093(2)	90	90
V/Å^3	288.50(14)	296.51(5)	306.64(4)	601.03(5)	603.74(6)
Z	2	2	2	4	4
Pearson symbol	*mP*20	*aP*20	*aP*20	*oP*40	*oP*40
$\rho_{calc.}$/g cm^{-3}	4.370	3.463	4.294	3.10	4.053
μ/mm^{-1}	23.703	5.200	29.278	2.5 42	18.743
Color	yellow	colorless	colorless	colorless	colorless
Crystal morphology	prism	block	block	block	block
Crystal size/mm^3	0.084 × 0.109 × 0.166	0.072 × 0.075 × 0.092	0.077 × 0.082 × 0.198	0.059 × 0.126 × 0.135	0.117 × 0.131 × 0.206
T/K	100	100	100	100	100
λ/Å	0.71073 (Mo-K_α)	0.71073 (Mo-K_α)	0.71073 (Mo-K_α)	0.71073 (Mo-K_α)	0.71073 (Mo-K_α)
No. of reflections	6587	6712	22457	32885	9729
θ range/°	3.64 to 30.54	3.682 to 32.178	3.599 to 32.691	3.530 to 35.052 °	3.541 to 35.027
Range of Miller indices	$-9 \le h \le 9$ $-7 \le k \le 7$ $-10 \le l \le 10$	$-7 \le h \le 7$ $-8 \le k \le 8$ $-15 \le l \le 15$	$-7 \le h \le 7$ $-8 \le k \le 8$ $-15 \le l \le 15$	$-16 \le h \le 16$ $-9 \le k \le 9$ $-16 \le l \le 16$	$-16 \le h \le 14$ $-9 \le k \le 9$ $-17 \le l \le 17$
Absorption correction	multi-scan	integration	multi-scan	multi-scan	multi-scan
$Trans._{max}$, $Trans._{min}$	0.24, 0.12	0.706, 0.646	0.143, 0.033	0.791, 0.721	0.213, 0.097
R_{int}, R_σ	0.0281, 0.0084	0.0532, 0.0558	0.0246, 0.0350	0.0269, 0.0084	0.0335, 0.0198
Completeness of the data set	0.998	0.989	0.999	0.998	0.999
No. of unique reflections	877	3930	2704	1335	1337
No. of parameters	47	96	94	48	48
No. of restrains	0	0	0	0	0
No. of constrains	0	0	0	0	0
S (all data)	1.255	0.935	1.059	1.255	1.243
$R(F)$ ($I \ge 2\sigma(I)$, all data)	0.0168, 0.0169	0.0363, 0.0542	0.0233, 0.0405	0.0158, 0.0181	0.0199, 0.0237
$wR(F^2)$ ($I \ge 2\sigma(I)$, all data)	0.0434, 0.0434	0.0880, 0.0936	0.0442, 0.0486	0.0360, 0.0367	0.0443, 0.0458
Extinction coefficient	not refined	not refined	not refined	0.0045(5)	0.0065(4)
$\Delta\rho_{max}$, $\Delta\rho_{min}$/e Å^{-3}	1.375, −1.710	1.853, −2.120	1.617, −1.943	0.473, −0.438	2.258, −1.658

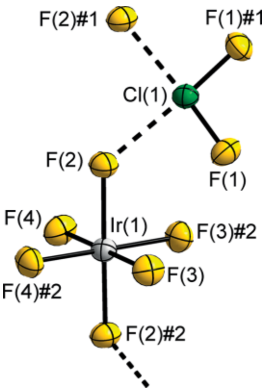

Figure 1. Section of the crystal structure of $ClF_2[IrF_6]$ showing the coordination spheres of the Cl and Ir atoms. Close contacts of F atoms to neighboring Cl atoms are shown as dashed bonds. Symmetry transformations: #1 1/2 – *x*, *y*, 3/2 – *z*, #2 3/2 – *x*, *y*, 3/2 – *z*. The displacement ellipsoids are shown at the 70 % probability level at 100 K.

*p*211.[33] The Cl and Ir atoms each form a pseudo cubic primitive lattice. The Cl atoms are thus surrounded by eight Ir atoms in the shape of a distorted cube when Cl–Ir distances of approximately 3.8–5.2 Å are considered, and vice versa for the Ir atoms. The Cl and Ir atoms are hence similarly arranged as the Cs and Cl atoms in the CsCl structure type.[36]

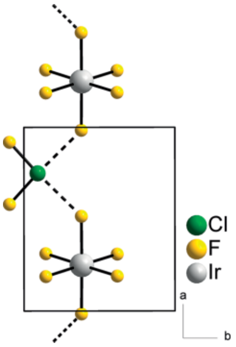

Figure 2. Crystal structure of $ClF_2[IrF_6]$ projected along the *c* axis. Close contacts of F atoms to neighboring Cl atoms are shown as dashed bonds. Atoms are shown with arbitrary radii.

The Crystal Structures of $ClF_2[SbF_6]$ and $ClF_2[BiF_6]$

The crystal structures of the isotypic salts difluorochloronium(III) hexafluoridoantimonate(V) and difluorochloronium(III) hexafluoridobismuthate(V) have been described previously.[10,25] The crystal structures were redetermined with higher precision of lattice parameters, atomic coordinates, bond lengths and angles. The space group was confirmed to be $P\bar{1}$ (No. 2). They crystallize with two formula units per unit cell, Pearson code *aP*20 and Wyckoff sequence 2.i^9*he*. See Table 1 for selected crystallographic data and details of the structure determinations. Atomic coordinates, equivalent isotropic and anisotropic displacement parameters, as well as a comparison with previously reported interatomic distances are given in the Supporting Information.

The chlorine atom occupies the Wyckoff position 2*i* (site symmetry 1) and is surrounded by the fluorine atoms F(1) and F(2), see Figure 3. The Cl–F bond lengths are 1.555(4) and 1.560(4) Å in $ClF_2[SbF_6]$ and 1.568(3) and 1.573(3) Å in $ClF_2[BiF_6]$, respectively. The F(1)–Cl(1)–F(2) angle is 97.0(2)° in the Sb and 95.9(2)° in the Bi compound. There are two symmetry-independent *M* (*M* = Sb, Bi) atoms in the unit cell: *M*(1) on position 1*h* and *M*(2) on position 1*e* (both site symmetries $\bar{1}$).

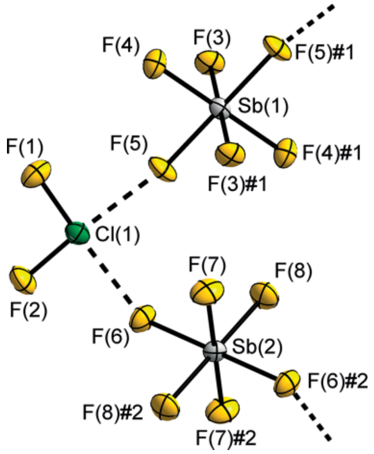

Figure 3. Section of the crystal structure of $ClF_2[SbF_6]$ showing the coordination spheres of the Cl and Sb atoms. Close contacts of F atoms to neighboring Cl atoms are shown as dashed bonds. Symmetry transformations: #1 1 – *x*, 1 – *y*, 1 – *z*, #2 1 – *x*, 1 – *y*, 2 – *z*. The displacement ellipsoids are shown at the 70 % probability level at 100 K. $ClF_2[BiF_6]$ is isotypic with $ClF_2[SbF_6]$.

The *M*(1) atom is surrounded by the fluorine atoms F(3) to F(5) and F(3)#1 to F(5)#1 in the shape of a slightly distorted octahedron. The *M*(2) atom is surrounded similarly by the fluorine atoms F(6) to F(8) and F(6)#2 to F(8)#2. The Sb–F bond lengths lie in the range of 1.862(3)-1.901(3) Å and the Bi–F bond lengths in the range of 1.956(3)-2.026(3) Å. By comparison, in $Li[SbF_6]$ the Sb–F bond length is 1.877(6) Å at room temperature and in $Ag[BiF_6]_2$ the Bi–F bond lengths lie in the range of 1.939(10)-2.048(9) Å at 298 K.[37,38] The crystal structures of other $A^{I}[BiF_6]$ salts are of insufficient quality to allow for proper comparison.

The fluorine atoms F(5) and F(6) of the $[MF_6]^-$ anions show short contacts to the chlorine atoms of 2.312(4) and 2.302(4) Å in the Sb and 2.252(3) and 2.254(3) Å in the Bi compound. The chlorine atom is surrounded by four fluorine atoms in a planar-quadrangular fashion (the distance of Cl(1) from the least-squares plane of the surrounding F atoms is 0.003(2) Å for $ClF_2[SbF_6]$ and 0.001(2) Å for $ClF_2[BiF_6]$). The resulting F(5)···Cl(1)···F(6) angle is 90.66(14)° in $ClF_2[SbF_6]$ and 90.88(12)° in $ClF_2[BiF_6]$.

When the short *M*–F···Cl contacts are taken into account, a zig-zag chain with *trans*-bridging $[MF_6]^-$ anions along the *c* axis results, see Figure 4. The zig-zag chains have the rod group symmetry $p\bar{1}$.[33] The Cl and *M* atoms each form a pseudo cubic primitive lattice. The Cl atoms are thus surrounded by eight *M* atoms in the shape of a distorted cube when Cl–*M* distances of approximately 3.9–5.2 Å are considered, and vice versa for *M*. The Cl and *M* atoms are consequently similarly arranged as the Cs and Cl atoms in the CsCl structure type.[36]

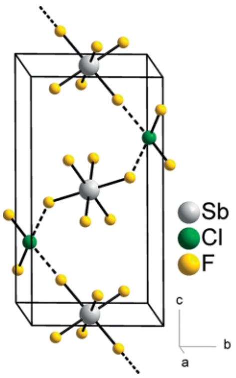

Figure 4. Crystal structure of $ClF_2[SbF_6]$. Close contacts of F atoms to neighboring Cl atoms are shown as dashed bonds. Atoms are shown with arbitrary radii. $ClF_2[BiF_6]$ is isotypic with $ClF_2[SbF_6]$.

The Crystal Structures of $ClF_2[NbF_6]$ and $ClF_2[TaF_6]$

The crystal structures of the isotypic salts difluorochloronium(III) hexafluoridoniobate(V) and difluorochloronium(III) hexafluoridotantalate(V) have been described previously.[23] The crystal structures were redetermined with higher precision of lattice parameters, atomic coordinates, bond lengths and angles. The space groups were confirmed to be *Pcca* (No. 54). They crystallize with four formula units per unit cell, Pearson symbol *oP*40 and Wyckoff sequence 54.f^4*de*. See Table 1 for selected crystallographic data and details of the structure determinations. Atomic coordinates, equivalent isotropic displacement parameters, anisotropic displacement parameters and a comparison with previously reported interatomic distances are given in the Supporting Information.

The chlorine atom occupies the Wyckoff position 4*d* (site symmetry 2) and is surrounded by the fluorine atom F(1) and a symmetry-generated F(1)#1 atom, forming the ClF_2^+ cation, see Figure 5. In $ClF_2[NbF_6]$, the Cl–F bond length is 1.571(1) Å and the F(1)–Cl(1)–F(1)#1 angle is 96.00(6)°. In $ClF_2[TaF_6]$, the respective values are 1.568(2) Å and 96.45(15)°. The *M* (*M* = Nb, Ta) atom occupies the 4*c* position (site symmetry 2) and is surrounded by six fluorine atoms, F(2) to F(4) and F(2)#2 to F(4)#2, in the shape of a distorted octahedron. The Nb–F bond lengths are 1.850(1)-1.949(1) Å and the Ta–F bond lengths are 1.862(2)-1.945(2) Å. In comparison, in the $Li[MF_6]$ salts the Nb–F distance is 1.863(3) Å and the Ta–F distance is 1.859(4) Å at 299 K.[35]

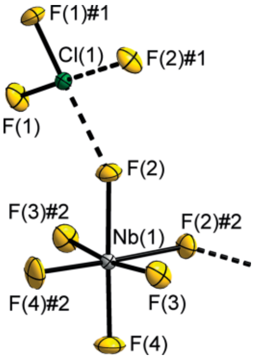

Figure 5. Section of the crystal structure of $ClF_2[NbF_6]$ showing the coordination spheres of the Cl and Nb atoms. Close contacts of F atoms to neighboring Cl atoms are shown as dashed bonds. Symmetry transformations: #1 1/2 – *x*, –*y*, *z*, #2 1 – *x*, *y*, 1/2 – *z*. The displacement ellipsoids are shown at the 70 % probability level at 100 K. $ClF_2[TaF_6]$ is isotypic with $ClF_2[NbF_6]$.

The fluorine atoms of the $[MF_6]^-$ anion (*M* = Nb, Ta), F(2) and F(2)#2, are *cis*-bridging to the Cl atoms with a distance of 2.234(1) Å and an angle F(2)•••Cl(1)•••F(2)#2 of 93.62(4)°. In the Ta compound the corresponding values are 2.252(2) Å and 93.47(10)°. This leads to significantly longer Nb(1)–F(2) and Ta(1)–F(2) bond lengths in comparison to the *M*–F bond lengths of non-bridging F atoms. The chlorine atom is thus surrounded by four fluorine atoms in a planar-quadrangular fashion (the distance of Cl(1) from the least-squares plane of the surrounding F atoms is 0 Å for both compounds, due to symmetry).

When the short *M*–F•••Cl contacts are taken into account, a helix with a translation period of *a* (9.9239(4) Å for Nb and 9.9577(6) Å for Ta) along the *a* axis results, see Figure 6. This helix can be described as a 2/1 helix with the rod group symmetry $p222_1$ (or p_a2_122 if *a* is taken as the unique rod group direction).[33] The isolated helix is chiral, but due to the symmetry of the space group, both *M* and *P* helices are present. The Cl and *M* (*M* = Nb, Ta) atoms each form a pseudo cubic primitive lattice. The Cl atoms are thus surrounded by eight *M* atoms in the shape of a distorted cube when Cl–*M* distances of approximately 4.1–5.2 Å are considered, and vice versa for *M* atoms. The Cl and *M* atoms are hence similarly arranged to the Cs and Cl atoms in the CsCl structure type.[36]

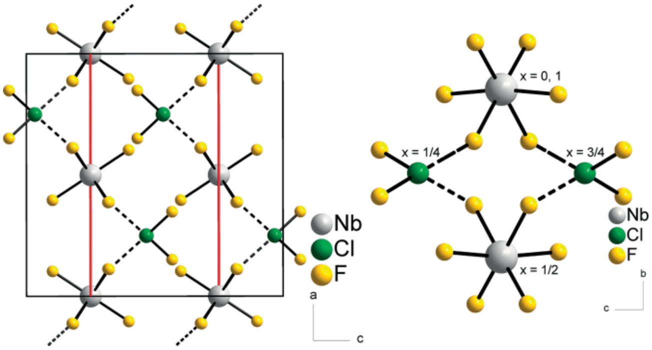

Figure 6. Left: section of the crystal structure of $ClF_2[NbF_6]$. The red lines indicate the spiral axes running along the 2_1 axes of the space group *Pcca* at *x*,0,1/4 (*P* helix) and *x*,1,3/4 (*M* helix). Right: projection of one *P* helix along its spiral axis parallel to the *a* axis. The *x* coordinates of the Cl and Nb atoms indicate the heights within the unit cell. Close contacts of F atoms to neighboring Cl atoms are shown as dashed bonds. Atoms are shown with arbitrary radii. $ClF_2[TaF_6]$ is isotypic to $ClF_2[NbF_6]$.

The Crystal Structure of $ClF_2[OsF_6]$

The reported crystal structure of $ClF_2[OsF_6]$ in the triclinic space group $P\bar{1}$ is questionable.[26] The authors first attempted the solution and refinement in the monoclinic space group *P*2/*m*, but then chose the space group $P\bar{1}$ instead, due to lower *R* values of the structural model. In the published structure, the ClF_2^+ ion is disordered, resulting in a too short Cl–F bond length of 1.38(7) Å. We observed that difluorochloronium(III) hexafluoridoosmate(V) crystallizes in the monoclinic space group *P*2/*c* (No. 13) with six formula units per unit cell, Pearson code *mP*60 and Wyckoff sequence 13.g^{14}*fe*. See Table 2 for selected crystallographic data and details of the structure determination.

Table 2. Selected crystallographic data and details of the structure determinations of difluorochloronium(III) fluoridometallates.

	$ClF_2[OsF_6]$	$ClF_2[RuF_6]$	$ClF_2[Ta_2F_{11}]$	$ClF_2[AuF_4]$
Formula	$ClOsF_8$	$ClRuF_8$	$ClF_{13}Ta_2$	$ClAuF_6$
Molar mass/g mol^{-1}	377.67	288.51	644.35	346.41
Space group (No.)	$P2/c$ (13)	$Pcca$ (54)	$P12_1/n1$ (14)	$P12_1/n1$ (14)
a/Å	15.584(2)	19.708(2)	7.6576(3)	4.4720(13)
b/Å	5.6370(9)	5.6153(6)	9.1844(4)	7.331(2)
c/Å	10.5162(16)	10.5024(12)	14.1108(6)	14.894(4)
α/°	90	90	90	90
β/°	107.903(2)	90	92.120(2)	97.580(5)
γ/°	90	90	90	90
V/Å^3	879.1(2)	1162.3(2)	991.74(7)	484.0(2)
Z	6	8	4	4
Pearson symbol	$mP60$	$oP80$	$mP64$	$mP32$
$\rho_{calc.}$/g cm^{-3}	4.280	3.298	4.316	4.754
μ/mm^{-1}	22.312	3.256	22.485	30.979
Color	colorless	pale green	colorless	pale yellow
Crystal morphology	prism	prism	block	prism
Crystal size/mm^3	0.223 × 0.290 × 0.310	0.080 × 0.100 × 0.150	0.093 × 0.096 × 0.139	0.010 × 0.030 × 0.180
T/K	100	143	100	100
λ/Å	0.71073 (Mo-K_α)	0.71073 (Mo-K_α)	0.71073 (Mo-K_α)	0.71073 (Mo-K_α)
No. of reflections	19970	14370	28468	11122
θ range/°	1.37 to 30.49	2.07 to 27.55 °	2.647 to 35.035	3.10 to 30.58
Range of Miller indices	$-14 \le h \le 14$	$-6 \le h \le 7$	$-12 \le h \le 12$	$-6 \le h \le 6$
	$-8 \le k \le 8$	$-13 \le k \le 13$	$-14 \le k \le 14$	$-10 \le k \le 10$
	$-20 \le l \le 20$	$-25 \le l \le 25$	$-22 \le l \le 22$	$-21 \le l \le 20$
Absorption correction	multi-scan	multi-scan	multi-scan	multi-scan
$Trans._{max}$, $Trans._{min}$	0.08, 0.06	0.78, 0.67	0.249, 0.135	0.75, 0.22
R_{int}, R_σ	0.0694, 0.0368	0.0246, 0.0147	0.0229, 0.0343	0.0625, 0.0432
Completeness of the data set	0.973	0.994	0.999	0.994
No. of unique reflections	2607	1339	4378	1482
No. of parameters	138	92	146	73
No. of restrains	0	0	0	0
No. of constrains	0	0	0	0
S (all data)	1.082	1.159	1.158	1.075
$R(F)$ ($I \ge 2\sigma(I)$, all data)	0.0423, 0.0483	0.0174, 0.0200	0.0184, 0.0228	0.0261, 0.0342
$wR(F^2)$ ($I \ge 2\sigma(I)$, all data)	0.1177, 0.1237	0.0435, 0.0444	0.0318, 0.0326	0.0632, 0.0658
Extinction coefficient	0.0016(3)	not refined	0.00207(5)	not refined
$\Delta\rho_{max}$, $\Delta\rho_{min}$/e Å^{-3}	3.641, −3.971	0.317, −0.546	1.156, −1.594	1.884, −1.372

Atomic coordinates, equivalent isotropic and anisotropic displacement parameters are reported in the Supporting Information.

There are two different kinds of chlorine atoms: Cl(1), Wyckoff position 2*e* (site symmetry 2) and Cl(2), position 4*g* (site symmetry 1), see Figure 7. The atom Cl(1) is surrounded by the fluorine atom F(1) and the symmetry-equivalent F(1)#1 atom with a Cl–F bond length of 1.567(5) Å and an F(1)–Cl(1)–F(1)#1 angle of 97.5(4)°. The atom Cl(2) is surrounded by the two fluorine atoms F(2) and F(3). The bond lengths are 1.572(5) and 1.576(5) Å and the F(2)–Cl(1)–F(3) angle is 97.0(3)°. The shapes of the two ClF_2^+ cations are equal within the tripled standard uncertainties.

The atom Os(1) occupies the 2*f* position (site symmetry 2) and is surrounded by six fluorine atoms, F(4) to F(6) and F(4)#2 to F(6)#2 in the shape of a distorted octahedron. The atom Os(2) occupies the 4*g* position (site symmetry 1) and is surrounded by the six fluorine atoms F(7) to F(12) in the shape of a distorted octahedron. The Os–F bond lengths in the $[Os(1)F_6]^-$ anion are 1.854(4)-1.910(4) Å and 1.852(4)-1.919(4) Å in the $[Os(2)F_6]^-$ anion. For comparison, the Os–F bond length in $Li[OsF_6]$ is 1.872(7) Å at 299 K.[35] In the previously reported crystal structure, the Os–F bond length was reported to be 1.84(3) Å.[26]

The Os(1)–F(6), Os(2)–F(7) and Os(2)–F(12) bond lengths are significantly longer than the other Os–F bond lengths, due to short contacts of the form Os–F•••Cl to the ClF_2^+ cations. These contacts are 2.288(4) Å for Cl(1)•••F(12), 2.260(5) Å for Cl(2)•••F(6) and 2.269(5) Å for Cl(2)•••F(7). The chlorine atoms are thus surrounded by four fluorine atoms in a planar-quadrangular fashion (the distances of the Cl atoms from the least-squares plane of the surrounding F atoms are 0 Å for Cl(1), due to symmetry, and 0.004(3) Å for Cl(2)). The angle F(12)•••Cl(1)•••F(12)#1 is 90.8(2)° and the F(6)•••Cl(2)•••F(7) is 90.0(2)°.

Severely deformed *M* and *P* 3/1 helices along the *a* axis with a translation period of *a* (15.584(2) Å) result, when Os–F•••Cl contacts are taken into account, see Figure 8.[34] Ideal 3/1 helices would have the rod group symmetries $p3_121$ and $p3_221$. As can be seen from the projection along the helix axis (right part of Figure 8), actually there exists no threefold screw axis and the rod group symmetry is only $p121$. The twofold rotation axes are perpendicular to the rod axis and run through the atoms Os(1) and Cl(1). The two kinds of chemical repeating units are not symmetry equivalent such that the equivalence postulate

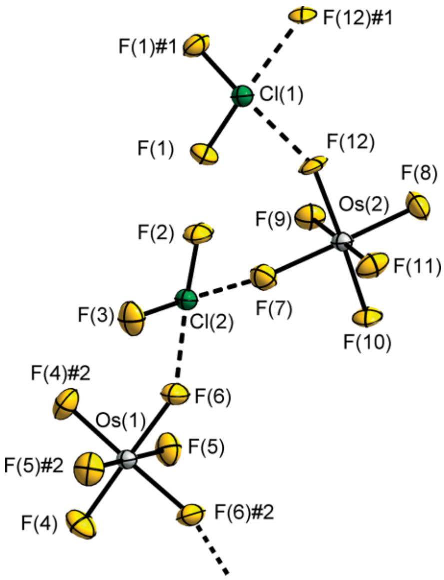

Figure 7. Section of the crystal structure of $ClF_2[OsF_6]$ showing the coordination spheres of the Cl and Os atoms. Close contacts of F atoms to neighboring Cl atoms are shown as dashed bonds. Symmetry transformations: #1 2 – *x*, *y*, 3/2 – *z*, #2 1 – *x*, *y*, 3/2 – *z*. The displacement ellipsoids are shown at the 70 % probability level at 100 K.

cannot be applied. The Cl and Os atoms each form a pseudo cubic primitive lattice. The Cl atoms are thus surrounded by eight Os atoms in the shape of a distorted cube when Cl–Os distances of approximately 3.8–5.2 Å are considered, and vice versa for Os. The Cl and Os atoms are consequently similarly arranged as the Cs and Cl atoms in the CsCl structure type.[36]

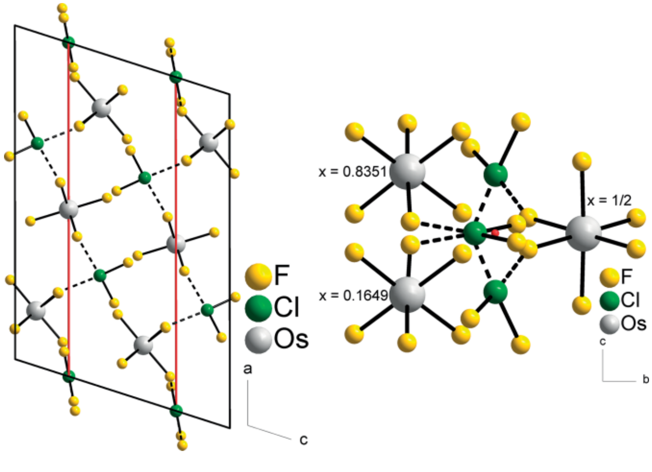

Figure 8. Left: section of the crystal structure of $ClF_2[OsF_6]$. The red lines indicate the spiral axes of two helices running along *x*,1/2,1/4 (*M* helix) and *x*,1/2,3/4 (*P* helix). Right: projection of one *P* helix along the *a* axis. For the sake of clarity, *x* coordinates indicating the height within the unit cell are only given for the Os atoms. Cl atoms are located at *x* = 0, 1/3, 2/3, 1. Close contacts of F atoms to neighboring Cl atoms are shown as dashed bonds. Atoms are shown with arbitrary radii.

The Crystal Structure of $ClF_2[RuF_6]$

The crystal structure of difluorochloronium(III) hexafluoridoruthenate(V) was redetermined.[24] The compound crystallizes in the orthorhombic space group *Pcca* (No. 54), Pearson code *oP*80 and Wyckoff sequence $54.f^{9}dc$. See Table 2 for selected crystallographic data and details of the structure determination. Atomic coordinates, equivalent isotropic and anisotropic displacement parameters, as well as a comparison with previously reported interatomic distances are given in the Supporting Information.

There are two symmetry-independent kinds of chlorine atoms: Cl(1), Wyckoff position 4*d* and Cl(2), position 4*c* (both site symmetry 2), Figure 9. The atom Cl(1) is surrounded by the fluorine atom F(1) and the symmetry-equivalent F(1)#1 atom. The atom Cl(2) is surrounded by the atom F(2) and the symmetry-equivalent F(2)#2 atom. For the $Cl(1)F_2^+$ cation a Cl–F bond length of 1.565(2) Å and an F(1)–Cl(1)–F(1)#1 angle of 96.80(13)° are observed. For $Cl(2)F_2^+$ they are 1.568(1) Å and 96.29(11)°. The values of the two ClF_2^+ cations are equal within the tripled standard uncertainties.

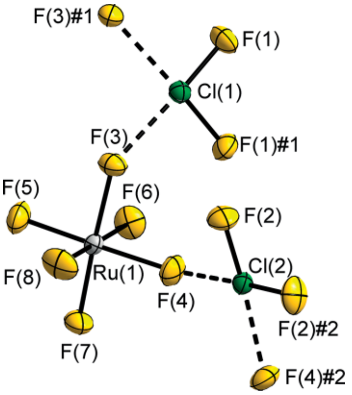

Figure 9. Section of the crystal structure of $ClF_2[RuF_6]$ showing the coordination spheres of the Cl and Ru atoms. Close contacts of F atoms to neighboring Cl atoms are shown as dashed bonds. Symmetry transformations: #1 1 – *x*, *y*, 3/2 – *z*, #2 1/2 – *x*, –*y*, *z*. The displacement ellipsoids are shown at the 70 % probability level at 143 K.

The Ru atom occupies the 8*f* position (site symmetry 1) and is surrounded by six fluorine atoms, F(3)–F(8), in the shape of a distorted octahedron. The Ru–F bond lengths are 1.819(1)-1.896(1) Å. For comparison, in $Li[RuF_6]$ the Ru–F bond length is 1.851(8) Å at 299 K.[35]

The atoms F(3) and F(4) of the $[RuF_6]^-$ anion show close contacts to the Cl atoms of the ClF_2^+ cations and thus have significantly longer Ru–F bond lengths of 1.896(1) and 1.891(1) Å, respectively. The resulting Cl···F distances are: Cl(1)···F(3): 2.271(1) Å; Cl(2)···F(4): 2.248(2) Å. The chlorine atoms are thus surrounded by four fluorine atoms in a planar-quadrangular fashion (the distances of the Cl atoms from the least-squares plane of the surrounding F atoms are 0 Å for both Cl atoms, due to symmetry). The angle F(3)···Cl(1)···F(3)#1 of 89.92(8)° is significantly smaller than the F(4)···Cl(2)···F(4)#2 angle of 91.25(7)°. Taking into account the Ru–F···Cl contacts, both *M* and *P* 4/1 helices with a translation period of *a* (19.708(2) Å) along the *a* axis result, see Figure 10.[34] The ideal rod group symmetries of the helices are $p4_122$ and $p4_322$. The penetration rod group of the helices in the crystal structure is $p222_1$. The Cl and Ru atoms each form a pseudo cubic primitive lattice. The Cl atoms are thus surrounded by eight Ru atoms in the shape of a distorted cube when Cl–Ru distances of 3.8–5.2 Å are considered, and vice versa for Ru. The Cl and Ru atoms are hence arranged similar to the Cs and Cl atoms in the CsCl structure type.[36]

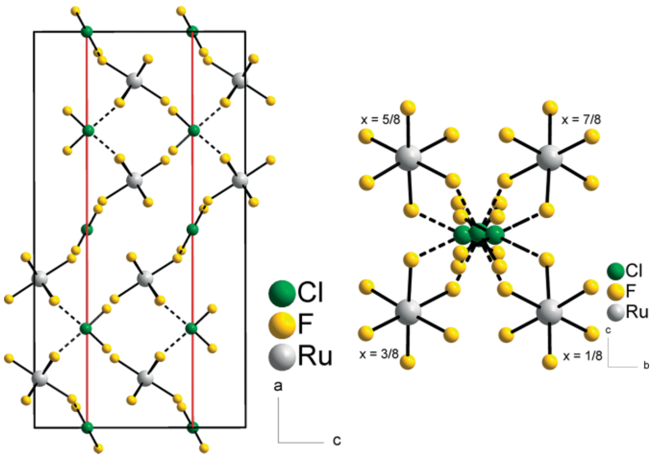

Figure 10. Left: section of the crystal structure of $ClF_2[RuF_6]$. The red lines indicate two spiral axes of two helixes running along *x*,1,1/4 (*M* helix) and *x*,1,3/4 (*P* helix). Right: projection of one *M* helix along the *a* axis. For the sake of clarity, idealized *x* coordinates indicating the heights within the unit cell are only given for the Ru atoms. Cl atoms are located at *x* = 0, 1/4, 1/2, 3/4, 1. Close contacts of F atoms to neighboring Cl atoms are shown as dashed bonds. Atoms are shown with arbitrary radii.

The Crystal Structure of $ClF_2[Ta_2F_{11}]$

Difluorochloronium(III) undecafluoridoditantalate(V) crystallizes in the monoclinic space group $P12_1/n1$ (No. 14), Pearson code *mP*64 and Wyckoff sequence $14.e^{16}$. See Table 2 for selected crystallographic data and details of the structure determination. Atomic coordinates, equivalent isotropic and anisotropic displacement parameters are reported in the Supporting Information.

The chlorine atom Cl(1) occupies the Wyckoff position 4*e* and is surrounded by the fluorine atoms F(1) and F(2), giving the ClF_2^+ cation (Figure 11). The Cl–F bonds lengths are 1.567(2) and 1.566(2) Å and the F(1)–Cl(1)–F(2) is 96.30(10)°. The two symmetry-independent Ta atoms, Ta(1) and Ta(2), both occupy the Wyckoff position 4*e*. The Ta(1) atom is surrounded by the terminal F atoms F(4) to F(8) and the Ta(2) atom by the atoms F(9) to F(13). The Ta–F bond lengths lie in the range of 1.835(2)-1.935(2) Å. The atom F(3) is μ-bridging between the two Ta atoms with bond lengths of 2.057(2) and 2.068(2) Å, giving the $[Ta_2F_{11}]^-$ anion, see Figure 11. The Ta–F bond lengths are comparable with the ones reported for $Cd[Ta_2F_{11}]_2$ of 1.821(4)-1.942(4) Å for terminal F atoms and 2.056(4)-2.077(4) Å for μ-bridging F atoms.[39]

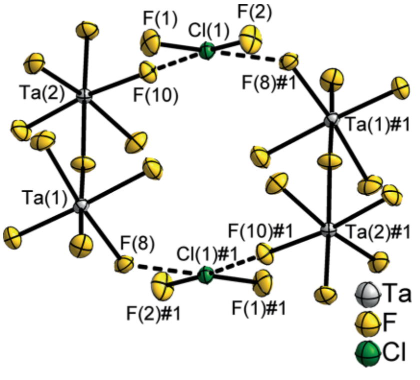

Figure 11. Molecular structure of the dimeric $ClF_2[Ta_2F_{11}]$. Symmetry transformation: #1 1 – *x*, 1 – *y*, 1 – *z*. The displacement ellipsoids are shown at the 70 % probability level at 100 K. Close contacts of F atoms to neighboring Cl atoms are shown as dashed bonds. Atom labels are only given for certain atoms for the sake of clarity.

The atoms F(8) and F(10) of the $[Ta_2F_{11}]^-$ anion show close contacts to the Cl atom and thus the corresponding Ta–F bond lengths of 1.935(2) and 1.934(2) Å are significantly longer than the other bond lengths of terminal F atoms. The resulting Cl···F bond lengths are: Cl(1)···F(8): 2.292(2) Å and Cl(1)···F(10): 2.235(2) Å. The angle F(8)···Cl(1)···F(10) is 92.89(6)°. Consequently, the Cl(1) atom is surrounded by four fluorine atoms in an almost planar, quadrangular fashion (the distance of Cl(1) from the least-squares plane of the surrounding F atoms is 0.017(1) Å).

When the Ta–F···Cl contacts are considered, a dimer of the form $(ClF_2[Ta_2F_{11}])_2$ results, see Figure 11. Each of the dimers is surrounded by twelve further dimers in the shape of a cuboctahedron, when center-to-center distances of approximately 7.6–9.4 Å are considered.

The Crystal Structure of $ClF_2[AuF_4]$

Difluorochloronium(III) tetrafluoridoaurate(III) crystallizes in the monoclinic space group $P12_1/n1$ (No. 14) with four formula units per unit cell, Pearson code *mP*32 and Wyckoff sequence $14.e^8$. See Table 2 for selected crystallographic data and details of the structure determination. Atomic coordinates, equivalent isotropic and anisotropic displacement parameters are reported in the Supporting Information. The chlorine atom occupies the Wyckoff position 4*e* (site symmetry 1) and is surrounded by the fluorine atoms F(1) and F(2), see Figure 12. The Cl–F bond lengths are 1.583(4) and 1.578(4) Å, respectively. The F(1)–Cl(1)–F(2) angle is 95.4(2)°.

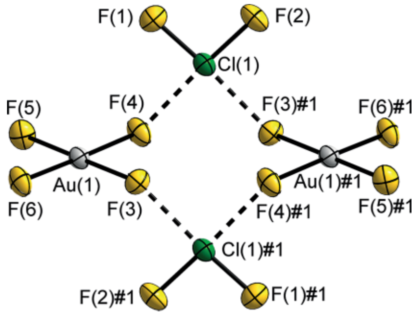

Figure 12. Molecular structure of the dimeric $ClF_2[AuF_4]$. Symmetry transformation: #1 –*x*, 1 – *y*, 1 – *z*. The displacement ellipsoids are shown at the 70 % probability level at 100 K. Close contacts of F atoms to neighboring Cl atoms are shown as dashed bonds.

The gold atom occupies the position 4*e* and is surrounded by four fluorine atoms F(3)–F(6), giving the nearly square-planar $[AuF_4]^-$ anion (the distance of Au(1) from the least-squares plane of the surrounding F atoms is 0.015(2) Å). The Au–F bond lengths lie in the range of 1.903(4)-1.961(4) Å. For comparison, those in $Li[AuF_4]$ are 1.890(7)-1.965(6) Å at room temperature.[40]

The bond lengths Au(1)–F(3) and Au(1)–F(4) are significantly longer than the other two Au–F bond lengths, due to close contacts to the Cl atom. The fluorine atoms of the $[\mathrm{AuF_4}]^-$ anions are *cis*-bridging and the Cl···F distances are 2.198(4) and 2.170(4) Å, respectively. The chlorine atom is thus surrounded by four fluorine atoms in an almost planar-quadrangular fashion (the distance of Cl(1) from the least-squares plane of the surrounding F atoms is 0.042(3) Å). The F(3)···Cl(1)···F(4) angle is 88.08(14)°.

When these Au–F···Cl contacts are considered, a dimer of the form $(\mathrm{ClF_2[AuF_4]})_2$ results, see Figure 12. Within this dimer, the $[\mathrm{AuF_4}]^-$ units lie in a plane and the $\mathrm{ClF_2}^+$ cations lie above and below this plane, leading to a "chair configuration" of the dimer. Each of the dimers is surrounded by eight further dimers in the shape of a hexagonal bipyramid, when center-to-center distances of approximately 4.5–8.3 Å are considered.

Quantum-Chemical Solid-State Calculations

The crystal structures of all our $\mathrm{ClF_2}^+$ compounds were investigated by quantum-chemical solid-state calculations using CRYSTAL17 (DFT-PBE0/TZVP level of theory).[41,42] The optimized structures are reported in the Supporting Information and a comparison of observed and calculated bond lengths, distances and angles are given in Table 3 to 5.

The calculated Cl–F bond lengths are with approximately 1.60 Å quite similar to the experimentally determined values but are 2 to 4 % longer. In contrast, the calculated Cl···F bridging distances are generally shorter and show a broad variation among the different compounds. The strength of the Cl–F bonds is thus somewhat underestimated by the used method and the strength of the Cl···F bridges is overestimated. The calculated F–Cl–F angles with circa 95.0° are also quite similar among all compounds and 1 to 8 % smaller than the experimentally determined ones. The calculated F···Cl···F angles show a broad variation and usually are bigger than the observed ones. The calculated *M*–F bond lengths are longer than the experimentally determined ones and thus the interactions with the cations are in comparison underestimated.

To get a qualitative picture of the bonding in these compounds, the atomic partial charges and overlap populations between atoms were examined by Mulliken analysis. The average atomic partial charges are reported in the Supporting Information and the average overlap populations (AOP) are given in Table 6.

The most negatively charged F atoms are the μ-bridging F atoms of the fluoridometallate anions, followed by the non-bridging F atoms. This agrees nicely with the observed *M*–F bond lengths. The AOPs for the Cl–F bonds of $\mathrm{ClF_2}^+$ are quite similar for all compounds and correlate well with the respective bond lengths. The AOPs for the Cl···F interactions are much smaller and support the assumption of a weak, mostly ionic interaction between Cl and the neighboring F atoms of the anions.

Table 3. Experimentally determined and calculated Cl–F bond lengths as well as Cl···F distances of the bridging F atoms of the fluoridometallate anions in difluorochloronium(III) fluoridometallates.

Compound	bridging mode	*d* exp./Å			*d* calcd. (DFT-PBE0/TZVP, solid-state)/Å	
		Cl–F	Cl···F	Reference	Cl–F	Cl···F
$\mathrm{ClF_2[AsF_6]}$	*trans*	1.541(14)	2.339(14)	[9]	1.59	2.28
$\mathrm{ClF_2[SbF_6]}$	*trans*	1.555(4), 1.560(4)	2.302(4), 2.312(4)	this work	1.60	2.26
$\mathrm{ClF_2[IrF_6]}$	*trans*	1.573(3)	2.300(3)	this work	1.61	2.24
$\mathrm{ClF_2[BiF_6]}$	*trans*	1.568(3), 1.573(3)	2.252(3), 2.254(3)	this work	1.60	2.21, 2.23
$\mathrm{ClF_2[NbF_6]}$	*cis*	1.571(1)	2.234(1)	this work	1.61	2.19
$\mathrm{ClF_2[TaF_6]}$	*cis*	1.568(2)	2.252(2)	this work	1.61	2.20
$\mathrm{ClF_2[RuF_6]}$	*cis*	1.565(2), 1.568(1)	2.248(2), 2.271(1)	this work	1.61	2.20, 2.23
$\mathrm{ClF_2[OsF_6]}$	*cis*	1.567(5), 1.572(5), 1.576(5)	2.260(5), 2.269(5), 2.288(4)	this work	1.60	2.22–2.25
$\mathrm{ClF_2[Ta_2F_{11}]}$	*cis*	1.566(2), 1.567(2)	2.235(2), 2.292(2)	this work	1.60	2.18, 2.26
$\mathrm{ClF_2[AuF_4]}$	*cis*	1.538(4), 1.578(4)	2.170(4), 2.198(4)	this work	1.61, 1.62	2.16, 2.18
$\mathrm{ClF_2[BF_4]}$	*cis*	1.562(1), 1.567(1)	2.270(1), 2.312(1)	[22]	1.60	2.24, 2.27

Table 4. Experimentally determined and calculated F–Cl–F angles as well as F···Cl···F angles of the bridging F atoms of the fluoridometallate anions in difluorochloronium(III) fluoridometallates.

Compound	bridging mode	∡ exp./°			∡ calcd. (DFT-PBE0/TZVP, solid-state)/°	
		F–Cl–F	F···Cl···F	Reference	F–Cl–F	F···Cl···F
$\mathrm{ClF_2[AsF_6]}$	*trans*	103.2(7)	93.7(5)	[9]	95.6	99.7
$\mathrm{ClF_2[SbF_6]}$	*trans*	97.0(2)	90.66(14)	this work	95.7	92.2
$\mathrm{ClF_2[IrF_6]}$	*trans*	97.1(2)	90.38(14)	this work	95.1	91.3
$\mathrm{ClF_2[BiF_6]}$	*trans*	95.90(19)	90.88(12)	this work	95.1	92.0
$\mathrm{ClF_2[NbF_6]}$	*cis*	96.00(6)	93.62(4)	this work	94.6	94.5
$\mathrm{ClF_2[TaF_6]}$	*cis*	96.45(15)	93.47(10)	this work	94.8	94.6
$\mathrm{ClF_2[RuF_6]}$	*cis*	96.29(11), 96.80(13)	89.92(8), 91.25(7)	this work	94.8, 95.6	89.4, 93.6
$\mathrm{ClF_2[OsF_6]}$	*cis*	97.0(3), 97.5(4)	90.0(2), 90.8(2)	this work	95.0, 95.8	92.6, 94.8
$\mathrm{ClF_2[Ta_2F_{11}]}$	*cis*	96.30(10)	92.89(6)	this work	94.9	95.1
$\mathrm{ClF_2[AuF_4]}$	*cis*	95.4(2)	88.1(1)	this work	94.5	88.3
$\mathrm{ClF_2[BF_4]}$	*cis*	96.42(5)	99.11(3)	[22]	95.0	101.4

Table 5. Experimentally determined and calculated *M*–F distances of non-bridging and bridging F atoms of the fluoridometallate anions in difluorochloronium(III) fluoridometallates.

Compound	bridging mode	*d* exp./Å			*d* calcd. (DFT-PBE0/TZVP, solid-state)/Å	
		M–F(non-bridging)	M–F(bridging)	Reference	M–F(non-bridging)	M–F(bridging)
$ClF_2[AsF_6]$	*trans*	1.637(16)-1.694(12)	1.740(13)	[9]	1.71–1.72	1.77
$ClF_2[SbF_6]$	*trans*	1.862(3)-1.868(3)	1.896(3)-1.901(3)	this work	1.88	1.94
$ClF_2[IrF_6]$	*trans*	1.860(3)-1.871(2)	1.913(3)	this work	1.86–1.87	1.92
$ClF_2[BiF_6]$	*trans*	1.956(3)-1.964(3)	2.019(3)-2.026(3)	this work	1.98	2.05–2.06
$ClF_2[NbF_6]$	*cis*	1.850(1)-1.871(1)	1.9494(7)	this work	1.87–1.89	1.98
$ClF_2[TaF_6]$	*cis*	1.862(2)-1.881(2)	1.945(2)	this work	1.88–1.90	1.99
$ClF_2[RuF_6]$	*cis*	1.819(1)-1.841(1)	1.891(1)-1.896(1)	this work	1.84–1.87	1.930
$ClF_2[OsF_6]$	*cis*	1.852(4)-1.875(5)	1.910(4)-1.919(4)	this work	1.87–1.90	1.96
$ClF_2[Ta_2F_{11}]$	*cis*	1.835(2)-1.886(2) 2.057(2)-2.068(2)[a]	1.934(2)-1.935(2)	this work	1.85–1.91 2.08–2.09[a]	1.97
$ClF_2[AuF_4]$	*cis*	1.903(4)-1.905(3)	1.950(3)-1.961(4)	this work	1.92–1.94	1.99–2.00
$ClF_2[BF_4]$	*cis*	1.375(2)-1.378(2)	1.421(2)-1.425(2)	[22]	1.36–1.38	1.43

[a] Value for the μ_2-F atom in the $[Ta_2F_{11}]^-$ anion.

Table 6. Average overlap population between two atoms from Mulliken population analysis of the optimized solid-state structures of difluorochloronium(III) fluoridometallates.

Compound	Bridging mode	average overlap population (DFT-PBE0/TZVP, solid-state)/*e*			
		Cl–F	Cl•••F	*M*–F(non-bridging)	*M*–F(bridging)
$ClF_2[AsF_6]$	*trans*	0.05	0.02	0.28	0.22
$ClF_2[SbF_6]$	*trans*	0.05	0.01	0.23	0.18
$ClF_2[IrF_6]$	*trans*	0.05	0.02	0.13	0.10
$ClF_2[BiF_6]$	*trans*	0.05	0.01	0.19	0.13
$ClF_2[NbF_6]$	*cis*	0.05	0.01	0.10	0.07
$ClF_2[TaF_6]$	*cis*	0.05	0.01	0.14	0.09
$ClF_2[RuF_6]$	*cis*	0.05	0.01	0.08	0.06
$ClF_2[OsF_6]$	*cis*	0.05	0.01	0.09	0.08
$ClF_2[Ta_2F_{11}]$	*cis*	0.06	0.01	0.12, 0.06[a]	0.09
$ClF_2[AuF_4]$	*cis*	0.03	0.01	0.10	0.08
$ClF_2[BF_4]$	*cis*	0.05	0.02	0.29	0.22

[a] Value for the μ_2-F atom in the $[Ta_2F_{11}]^-$ anion.

Overall, the anion has a minor impact on the calculated structural parameters of the ClF_2^+ cation, whereas the nature of the bridging *M*–F•••Cl contacts depends much more on the anion.

Quantum-Chemical Modeling of the Fluorine-Bridging Effect in the Gas-Phase

As has been previously shown in a detailed study of the closely related $ClF_4[SbF_6]$ salt, its anion-cation interactions strongly impact the structure.[43] Quantum-chemical modeling of this effect presented a major challenge. The assumption of simple ion pairs alters the nature of the fluorine bridges, and the modeling of infinite chains is computationally prohibitive. The use of trinuclear fragments with either ClF_4^+ or $[SbF_6]^-$ in the center results in incorrect overall charges, and chain termination becomes a major problem. The best approximation found for $ClF_4[SbF_6]$ was the use of ClF_4^+ capped by two neutral HF molecules with the Cl•••F bridge bond length, observed in the crystal structure, used as the only constraint. This approach preserved the positive charge on ClF_4^+ and reduced the computational requirements.

In the present study, either trinuclear species with ClF_2^+ in the center of the form $[ClF_2[MF_6]_2]^-$ (*M* = Nb, Ta, Ru, Os, Ir, As, Sb, Bi) or dimers ($(ClF_2[Ta_2F_{11}])_2$, $(ClF_2[AuF_4])_2$, $(ClF_2[BF_4])_2$) were investigated by means of quantum-chemical gas-phase calculations with TURBOMOLE (DFT-PBE0/def2-TZVP level of theory).[44,45] The *xyz* coordinates of the optimized molecular structures, selected bond lengths, angles as well as partial atomic charges from a natural population analysis are reported in the Supporting Information.[46]

As can be seen from Table 8, the molecular structure of ClF_2^+ observed in the crystal structures is in excellent agreement with that predicted by high-level quantum chemical calculations at the CCSD(T) level for the free gaseous ion.[47] The DFT calculations for the solid salts are in fair agreement with the experimental crystallographic values but overestimate the Cl–F bond lengths and therefore underestimate the F–Cl–F bond angle. The DFT calculations for the gaseous state, using the trinuclear $[ClF_2[MF_6]_2]^-$ anion model, result in the same Cl–F bond length as the solid state calculations but show a further compression of the F–Cl–F bond angle. As for $ClF_4[SbF_6]$, the HF terminated ClF_2^+ model, $[ClF_2(HF)_2]^+$ gave the best results.

Atomic charges from natural population analyses show that the bridging F atoms of the fluoridometallate anions are usually the most negatively charged ones. They are followed by the non-bridging F atoms and the F atoms of the ClF_2^+ cation. The latter ones are the least negatively charged ones and the values are similar among the different bonding models, indicating only minor effects of the anions.

Bonding in the ClF_2^+ Cation

Halogen fluorides offer a golden opportunity to study the influence of oxidation state, coordination number and sterically active free valence electron pairs on the structure and bonding.[4] Their oxidation states range from +1 to +7, they are amphoteric, capable of forming cations and anions, and in most cases possess sterically active free valence electron pairs and hyper valency. The only exceptions are ClF and ClF_2^+ which are not hypervalent, ClF_6^+ which does not possess a free valence electron pair, and $[ClF_6]^-$ which has a free valence electron pair, but which is sterically inactive.[48,49]

The underlying structural principles are rather simple.[4] When the Cl atom has a free valence electron pair, it seeks maximal *s* character to stay as close as possible to the nucleus. If the coordination number exceeds four, so many Cl–F bonds will form semi-ionic, three-center four-electron bonds, until the free pair can participate in a more desirable sp^n hybrid orbital. As a result, chlorine fluorides can possess two different kinds of Cl–F bonds, shorter, strong, mainly covalent bonds and longer, weaker, semi-ionic, 3c-4e bonds.

As already mentioned above, ClF_2^+ has two free valence electron pairs and is not hypervalent. Therefore, it can easily form an sp^3 hybrid orbital involving the two strong Cl–F bonds and the two free valence electron pairs, resulting in a pseudo-tetrahedral structure. The coordination sphere around the Cl atom is extended by two more, highly ionic fluorine bridges from neighboring anions. These fluorine bridges avoid the free valence electron pairs of the Cl atom and approach it in the ClF_2 plane, resulting in a total coordination number of six. It must be pointed out, however, that the two free valence electron pairs do not occupy the linear axial positions of an AX_4E_2-type VSEPR octahedron, as is present for example in $[ClF_4]^-$, but are strongly bent because they are part of the underlying AX_2E_2 pseudo-tetrahedron.[4,50]

Evidence for electron localization can be obtained computationally using, for example, the ELF (electron-localization function), the HELP (the High Electron Localization domain Population), or the MESP (molecular electrostatic potential) to "observe" increased electron density in the corresponding electron density basins.[51–53] HELP is a theoretically well defined (but non unique) qualitative measure of the number of localized and delocalized electrons in a region of space.[51,53] The ELF approach was chosen in our case for ClF_2^+ in the gaseous trinuclear $[ClF_2[SbF_6]_2]^-$ anion (Figure 13) and shows increased electron density in the basins attributed to the free valence electron pairs.[54,55] The ELF also shows the differences between the strong, polar covalent Cl–F bonds within the ClF_2^+ cation and the weak, highly ionic Cl•••F bridge bonds.

Two attractors, that is maxima of ELF, which are located above and below the ClF_2^+ plane, are found, which correspond to the two lone pairs of the Cl(III) atom in the Lewis picture. These lone pair domains were further analyzed by intra-basin partitioning of ELF (HELP and the High Electron Localization domain Volume (HELV)), see Table 7.[51] Among the investigated species the HELP values are similar with approximately 1.50 *e* per domain and the corresponding volumes of the localized electrons are circa 16 Bohr^3, which indicates that the different anions have minor effects on the lone pairs of the Cl(III) atom. For comparison, the values around 1.5 electrons are close to the value obtained for PH_3, lower than that of NH_3, and larger than that of AsH_3.[53]

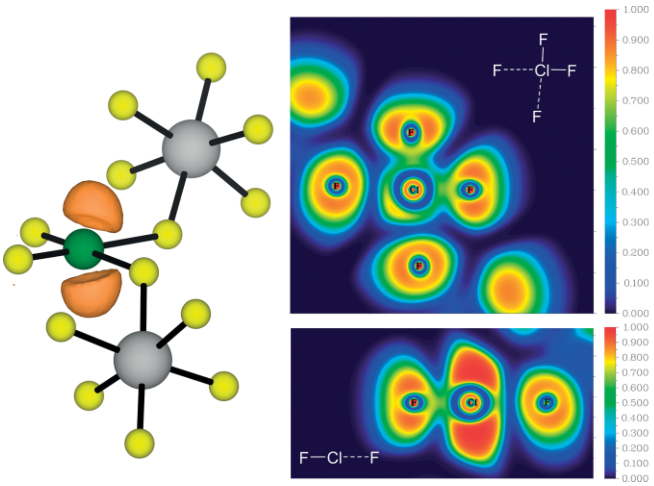

Figure 13. Left: projection of the three-dimensional ELF (orange) of $[ClF_2[SbF_6]_2]^-$ with $\eta(r) = 0.9$. The Cl atom is shown in green, the Sb atoms in grey and the F atoms in yellow. Right: projections of the ELF of $[ClF_2[SbF_6]_2]^-$ of certain planes. The corresponding planes are indicated in white in the top right or bottom left corner. Top: section through the plane of the ClF_2^+ cation, showing the ClF_2^+ cation and two bridging F atoms of $[SbF_6]^-$ units close to the Cl atom. Bottom: section through the plane of F–Cl•••F.

Table 7. Average high electron localization domain population (HELP) and average high electron localization domain volume (HELV) of the lone pair domains of the Cl atoms of ClF_2^+ in the optimized gas-phase, model structures of difluorochloronium(III) fluoridometallates.[51]

Model (Point group)	HELP/*e*	HELV/Bohr^3
$[ClF_2[AsF_6]_2]^-$ (C_2)	1.50	15.9
$[ClF_2[SbF_6]_2]^-$ (C_1)	1.50	16.0
$[ClF_2[BiF_6]_2]^-$ (C_1)	1.51	16.1
$[ClF_2[IrF_6]_2]^-$ (C_2)	1.52	15.7
$[ClF_2[NbF_6]_2]^-$ (C_2)	1.50	16.1
$[ClF_2[TaF_6]_2]^-$ (C_2)	1.50	16.3
$[ClF_2[RuF_6]_2]^-$ (C_2)	1.50	15.8
$[ClF_2[OsF_6]_2]^-$ (C_1)	1.50	16.0
$[ClF_2[Ta_2F_{11}]]_2$ (C_i)	1.50	16.4
$[ClF_2[AuF_4]]_2$ (C_i)	1.52	17.2
$[ClF_2[BF_4]]_2$ (C_i)	1.51	16.9
ClF_2^+ (C_{2v})	1.61	27.2
$[ClF_2(HF)_2]^+$ (C_2)	1.53	19.7

General Remarks on the Crystal Structures of Difluorochloronium(III) Compounds

In the investigated and the previously reported difluorochloronium(III) compounds, the structures of the ClF_2^+ cations are similar with only minor differences in the Cl–F bond lengths and F–Cl–F bond angles (Table 8). The Cl atoms are always coordinated by two additional F atoms from neighboring fluoridometallate anions, resulting in almost planar-quadrangular or planar-quadrangular planes.

Table 8. Comparison of the experimentally determined bond lengths and bond angles of ClF_2^+ with those calculated for the free gaseous cation, the solid salts, the gaseous trinuclear $[ClF_2[MF_6]_2]^-$ anions, and the gaseous $[ClF_2(HF_2)_2]^+$ cation.

Source	d(Cl–F)/Å	∡ F–Cl–F/°
Experimentally determined from crystal structures	1.54–1.57	95.9–103.2
Free, gaseous ClF_2^+ (CCSD(T)/aug-cc-pVTZ)[47]	1.552	101.7
Free, gaseous ClF_2^+ (DFT-PBE0/def2-TZVP)	1.54	102.5
Solid ClF_2^+ salts (DFT-PBE0/TZVP)	1.59–1.61	94.6–95.7
Gaseous $[ClF_2[MF_6]_2]^-$ (DFT-PBE0/def2-TZVP)	1.59–1.61	91.0–91.9
Gaseous $[ClF_2(HF_2)_2]^+$ (DFT-PBE0/def2-TZVP)	1.55	98.0

Inspection of the Cl···F distances and F···Cl···F angles shows that they strongly vary with the fluoridometallate anion. The *M*–F···Cl interactions lead to either the formation of molecular building units in $(ClF_2[BF_4])_2$, $(ClF_2[AuF_4])_2$ and $(ClF_2[Ta_2F_{11}])_2$, or to chains in $ClF_2[MF_6]$, *M* = Nb, Ta, Ru, Os, Ir, As, Sb, Bi.[9,22]

For compounds containing $[MF_6]^-$ anions, either *cis-* or *trans*-bridging of the F atoms is observed, but not both. When the $[MF_6]^-$ anions are *trans*-bridging (*M* = Ir, As, Sb, Bi), either linear (*M* = Ir), or zig-zag chains (*M* = As, Sb, Bi) are formed.[9] If the $[MF_6]^-$ anions are *cis*-bridging, chains with different shapes are formed. The chains are chiral, but both left- and right-handed chains are present, yielding racemates due to the centrosymmetric crystal structures. They are 2/1 helices for the Nb and Ta compounds and 4/1 helices for the Ru compound. For $ClF_2[OsF_6]$, the chain can be described as a severely deformed 3/1 helix. Regardless of the bridging-type, a pseudo-cubic primitive arrangement of the Cl and *M*(V) atoms is observed for all $ClF_2[MF_6]$ compounds, corresponding to the CsCl structure type. The observed crystal structures show no correlation with the effective ionic radii of the *M*(V) ions.[56] The two compounds with the smallest and biggest effective ionic radii of the M(V) atoms, As(V) and Bi(V), show a zig-zag chain structure.[56] One could argue that in contrast to that, the bridging type of the $[MF_6]^-$ polyhedra might be correlated with the electronegativity (χ_{AR}) of the central atom, as *trans*-bridging is observed for the compounds containing the more electronegative elements (As, Sb, Bi, Ir), while *cis*-bridging is observed for those with the less electronegative ones (Nb, Ta, Ru, Os).[57,58] However, this correlation with electronegativity is not valid as *cis*-bridging Ru and Os and *trans*-bridging Ir have quite similar electronegativity values. Valence electron configuration of the *M*(V) atoms also does not play a clear role. So, one can only speculate what driving forces are responsible for the differences in the crystal structures.

Conclusion

The difluorochloronium(III) compounds $ClF_2[MF_6]$ (*M* = Nb, Ta, Ru, Os, Ir, Sb, Bi), $ClF_2[Ta_2F_{11}]$, and $ClF_2[AuF_4]$ have been synthesized from reactions of metals, fluorides or chlorides with chlorine trifluoride. A similarly shaped ClF_2^+ cation is present in the crystal structures of all investigated compounds. This cation has two strong, short, mainly covalent Cl–F bonds, and two sterically active, free valence electron pairs in a pseudo-tetrahedral arrangement.[59] The coordination around the Cl atom is extended by two highly ionic, long fluorine bridges to neighboring fluoridometallate anions, resulting in a total coordination number of six. Regardless of the anion, the Cl atom and the four fluorine ligands form a perfect or almost perfect quadrangular plane. The bridging-modes of the $[MF_6]^-$ anions show neither a clear correlation with the effective ionic radii of the *M* atoms nor with their electronegativity. Quantum-chemical solid-state and gas-phase calculations were carried out and are in accord with the experimentally determined structures.

Experimental Section

General: Volatile materials were handled in either a Monel metal Schlenk line or a stainless steel/Teflon-FEP vacuum line, which were passivated with 100 % fluorine and/or chlorine trifluoride at various pressures before use.[5,60] Moisture-sensitive compounds were stored and handled in Ar- or N_2-filled glove boxes (MBraun, Vacuum Atmospheres Co). Reaction vessels were made of fluoropolymer (PFA or Teflon-FEP) or stainless steel (Hoke) that were closed by stainless steel valves. All reactors were passivated with fluorine or ClF_3 before use. Preparations were carried out in an atmosphere of dry and purified argon (5.0, Praxair). Chlorine trifluoride was stored over NaF to remove any traces of HF. Caution! *Fluorine, chlorine trifluoride, and difluorochloronium(III) compounds are strong oxidative fluorinators. They react explosively upon hydrolysis or contact with organic materials and must be handled using appropriate protective gear.*

Synthesis

$ClF_2[RuF_6]$, $ClF_2[OsF_6]$, $ClF_2[IrF_6]$, $ClF_2[AuF_4]$: A passivated 30 mL stainless steel cylinder was loaded outside the glove box with 1.0 mmol of the corresponding metal powder. The cylinder was connected to the stainless-steel vacuum line, evacuated and an excess of ClF_3 (5.0 g, 54 mmol) condensed in at 77 K. The reactor was warmed to room temperature over a period of two hours. After 8 hours, all volatile materials (ClF and ClF_3) were slowly pumped off. The ClF_2^+ salts were isolated as crystalline solids ($ClF_2[RuF_6]$ isolated: 281 mg, calculated 289 mg; $ClF_2[OsF_6]$ isolated: 375 mg, calculated 378 mg; $ClF_2[IrF_6]$ isolated: 377 mg, calculated 380 mg; $ClF_2[AuF_4]$ isolated: 342 mg, calculated 346 mg).

$ClF_2[NbF_6]$, $ClF_2[SbF_6]$, $ClF_2[TaF_6]$, $ClF_2[Ta_2F_{11}]$, $ClF_2[BiF_6]$: A PFA reaction vessel was loaded with the metal starting material in the glove box and attached to a stainless-steel valve. An excess of ClF_3 was then condensed onto the solid at 77 K. The vessel was warmed slowly to room temperature. The unreacted ClF_3 and ClF by-product were then slowly pumped off, and the colorless residue was removed in the glove box. $ClF_2[NbF_6]$: 20.6 mg of NbF_5 (0.11 mmol) was treated with approximately 0.07 g (0.8 mmol) of ClF_3. Volatiles were pumped off after a few hours at room temperature (29.2 mg isolated, calculated: 30.8 mg). $ClF_2[SbF_6]$: 0.407 g of SbF_3 (2.3 mmol) was treated with approximately 3 g (32 mmol) of ClF_3. Volatiles were removed after one hour at room temperature (0.641 g isolated, calculated: 0.704 g). $ClF_2[TaF_6]$: 21.0 mg of $TaCl_5$ (0.059 mmol) was treated with approximately 0.13 g (1.4 mmol) of ClF_3. Volatiles were removed after a few hours at room temperature. (19.0 mg isolated, 21.7 mg calculated). $ClF_2[Ta_2F_{11}]$: 29.6 mg of $TaCl_5$ (0.083 mmol) was treated with approximately 0.09 g (1 mmol) of ClF_3. Volatiles were removed after a few hours at room temperature. Crystals of both, $ClF_2[TaF_6]$ and $ClF_2[Ta_2F_{11}]$, were present in the product (29.7 mg isolated). $ClF_2[BiF_6]$: 35.2 mg of BiF_5 (0.12 mmol) was treated with approximately 0.09 g (1 mmol) of ClF_3. Volatiles were removed after a few hours at room temperature (40.9 mg isolated, calculated: 47.6 mg).

Single-Crystal X-ray diffraction: Crystals of the moisture-sensitive compounds were selected under dried perfluorinated oil (Fomblin YR1800, Solvay, stored over molecular sieves 3 Å) and mounted on a MiTeGen loop. Intensity data of suitable crystals were recorded with a D8 Quest diffractometer (Bruker), an APEX II DUO diffractometer (Bruker) or an IPDS2 diffractometer (STOE). The diffractometers were operated with monochromatized Mo-K_{α} radiation (0.71073 Å), multi-layered optics (D8 Quest), a TRIUMPH curved crystal (APEX II DUO) or a graphite monochromator (IPDS2) and equipped with a PHOTON 100 CMOS detector (D8 Quest), a CCD detector (Apex II DUO) or an image plate detector (IPDS2). Evaluation, integration and reduction of the diffraction data was carried out with the APEX3 software suite (D8 Quest and Apex II DUO) or the X-Area software suite (IPDS2).[61,62] The diffraction data were corrected for absorption utilizing the multi-scan method of SADABS or TWINABS within the APEX3 software suite (D8 Quest and Apex II DUO) or the integration method with the modules X-Shape and X-Red32 of the X-Area software suite (IPDS2T). The structures were solved with dual-space methods (SHELXT) and refined against F^2 (SHELXL).[63,64] Systematic absence violations were observed for the space groups of the compounds $ClF_2[MF_6]$ (M = Nb, Ta, Ru, Os, Ir) and $ClF_2[Ta_2F_{11}]$. However, the very weak intensities of the corresponding reflections were very close to the tripled standard uncertainties. Solution and refinement of the structures in crystallographic subgroups resulted in significant correlations between atomic coordinates and non-positive definite displacement parameters for some atoms. The crystal structures were consequently solved and refined in the space groups reported here, which were also indicated by the Addsym feature of the program package PLATON when checking for additional symmetry within the subgroups.[65,66] The crystals of $ClF_2[SbF_6]$ and $ClF_2[BiF_6]$ used for the diffraction experiment were non-merohedral twins (three twin components in $ClF_2[SbF_6]$ and two twin components in $ClF_2[BiF_6]$). The lattice parameters and twin law of $ClF_2[BiF_6]$ were determined with the program CELL_NOW.[67] In the case of $ClF_2[SbF_6]$, the twin components were determined manually in the X-Area software. In both cases only the non-overlapping reflections of the major twin component were used for the structure solution. The data were initially refined with the HKLF5 format option in SHELXL with all reflections (overlapping reflections and non-overlapping reflections of all twin components). The data were then processed with the HKLF5Tools program: the non-overlapping reflections of the weaker diffracting twin component were removed, the non-overlapping reflections of the major twin component were merged in point group $\bar{1}$ and the overlapping reflections were merged in point group 1.[68] In the case of $ClF_2[BiF_6]$ the final refinement was carried out against the detwinned dataset (created by SHELXL with the LIST 8 option as a FCF file and converted to a HKL file with HKLF5Tools). The locations of highest residual electron densities after the final refinement were the following: $ClF_2[IrF_6]$: 0.78 Å from atom Ir(1), $ClF_2[SbF_6]$: 0.68 Å from atom Sb(2), $ClF_2[BiF_6]$: 0.82 Å from atom Bi(1), $ClF_2[NbF_6]$: 0.74 Å from atom Cl(1), $ClF_2[TaF_6]$: 0.70 Å from atom Ta(1), $ClF_2[OsF_6]$: 0.81 Å from atom Os(2), $ClF_2[RuF_6]$: 1.28 Å from atom F(3), $ClF_2[Ta_2F_{11}]$: 1.79 Å from atom F(7), $ClF_2[AuF_4]$: 1.13 Å from atom Au(1). Representations of the crystal structures were created with the Diamond software.[69]

Deposition Numbers 2008578–2008586 contain the supplementary crystallographic data for this paper. These data are provided free of charge by the joint Cambridge Crystallographic Data Centre and Fachinformationszentrum Karlsruhe Access Structures service www.ccdc.cam.ac.uk/structures.

Solid-State Quantum-chemical Calculations: Periodic quantum-chemical calculations were carried out for difluorochloronium(III) fluoridometallates with the PBE0 hybrid density functional method (DFT-PBE0).[41,42] Triple-zeta-valence + polarization (TZVP) level basis sets were applied for all atoms. Details of the used basis sets are given in the Supporting Information. All calculations were carried out with the CRYSTAL17 program package.[70] The crystal structures of $ClF_2[AsF_6]$ and $ClF_2[BF_4]$ were taken from previous studies.[9,22] The reciprocal space was sampled with the following Monkhorst-Pack-type k-point grids: $ClF_2[AsF_6]$: 2×3×3, $ClF_2[IrF_6]$: 4×5×3, $ClF_2[SbF_6]$: 5×5×3, $ClF_2[BiF_6]$: 5×5×3, $ClF_2[NbF_6]$: 3×5×3, $ClF_2[TaF_6]$: 3×5×3, $ClF_2[OsF_6]$: 2×4×2, $ClF_2[RuF_6]$: 1×5×2, $ClF_2[Ta_2F_{11}]$: 3×3×2, $ClF_2[AuF_4]$: 5×3×2, $ClF_2[BF_4]$: 4×3×3. For the evaluation of the Coulomb and exchange integrals (TOLINTEG), tight tolerance factors of 8, 8, 8, 8, 16 were used for all calculations. Both the atomic positions and lattice parameters were fully optimized within the constraints imposed by the space group symmetry. Default DFT integration grids and optimization convergence thresholds were applied in all calculations. Mulliken population analyses were carried out for all compounds. For the magnetic systems $ClF_2[MF_6]$ (M = Ru, Os, Ir) a ferromagnetic ground state was employed. The resulting magnetic moments were 2.0 μB for the $[IrF_6]^-$ anion (1.4 μB contribution from Ir), 3.0 and 2.9 μB for the two independent $[OsF_6]^-$ anions (2.4 μB contribution from the respective Os atom) and 3.0 μB for the $[RuF_6]^-$ anion (2.3 μB contribution from Ru).

Gas-Phase Quantum-chemical Calculations: Gas-phase quantum-chemical calculations were carried out with the TURBOMOLE program package (version 7.2.1) using the PBE0 hybrid density functional method and Karlsruhe triple-zeta-valence + polarization basis sets (def2-TZVP).[44,45,71] The basis sets of Nb, Ru and Sb include a 28-electron scalar relativistic effective core potential. The basis sets of Ta, Ir, Au, Bi include a 60-electron scalar relativistic effective core potential. The resolution-of-the-identity technique was used to speed up the calculations.[72,73] For the magnetic systems $[ClF_2[MF_6]_2]^-$ (M = Ir, Os, Ru) magnetic ground states were employed. The resulting magnetic moments from natural population analyses were 2.0 μB for the $[IrF_6]^-$ anion (1.5 μB contribution from Ir), 3.0 μB for each of the $[OsF_6]^-$ anions (2.4 μB contribution from the respective Os atom) and 3.0 μB for the $[RuF_6]^-$ anion (2.4 μB contribution from Ru). All calculations were done in the gas phase without any solvent models. A full geometry optimization was carried out in the stated point group. All structures were confirmed to be true local minima by harmonic frequency calculations. Natural population analyses were carried out with the scheme implemented in Turbomole.[46] Electron localization functions (ELF) were generated with the program package Multiwfn (version 3.7).[54,74] A 300×300 grid was used for the generation of color-coded maps and a high-quality grid for the three-dimensional electron localization functions. The figure of the three-dimensional ELF was generated with the program package VESTA (version 3).[75,76] Analyses of the high electron localization domain population (HELP) and high electron localization domain volume (HELV)) were carried out with Multiwfn, medium-quality grids and standard settings were used for the basin analysis.[51]

Acknowledgments

We thank the Deutsche Forschungsgemeinschaft (DFG) for generous funding and another chemist, who wants to remain anonymous, for the donation of some ClF_3. We thank Prof. Dr. Martin Rahm, Chalmers University of Technology Gothenburg, Sweden for helpful discussions on HELP and HELV. Open access funding enabled and organized by Projekt DEAL.

Keywords: Difluorochloronium(III) cation · Chlorine trifluoride · Fluorine chemistry · Single-crystal X-ray diffraction

[1] O. Ruff, H. Krug, *Z. Anorg. Allg. Chem.* **1930**, *190*, 270–276.
[2] *Interhalogen Handbook, Technical Report AFRPL-TR-67–276*, Rocketdyne, Canoga Park, *California*, **1967**.
[3] J. VanOmmeren, *J. ASTM Int.* **2009**, *6*, JAI102215.
[4] K. O. Christe, in *XXIVth International Congress of Pure and Applied Chemistry*, Butterworth-Heinemann, Oxford, **1974**, pp. 115–141.
[5] R. Haiges, in *Efficient Preparations of Fluorine Compounds* (Ed.: H. W. Roesky), John Wiley & Sons, Inc., Hoboken, NJ, USA, **2012**, pp. 100–107.
[6] L. Stein, R. C. Vogel, *Ind. Eng. Chem.* **1956**, *48*, 418–421.
[7] W. Bacher, E. Jacob (Eds.), *Gmelin-Handbuch Der Anorganischen Chemie Teil*: System-Nr. 55., U. Uran, Ergänzungsband C8: *Verbindungen Mit Fluor*, Springer-Verlag, Berlin Heidelberg New York, **1980**.
[8] R. Bougon, B. Buu, K. Seppelt, *Chem. Ber.* **1993**, *126*, 1331–1336.
[9] H. Lynton, J. Passmore, *Can. J. Chem.* **1971**, *49*, 2539–2543.
[10] A. J. Edwards, R. J. C. Sills, *J. Chem. Soc. A* **1970**, 2697–2699.
[11] K. O. Christe, A. E. Pavlath, *Z. Anorg. Allg. Chem.* **1965**, *335*, 210–216.
[12] M. Schmeißer, W. Ludovici, D. Naumann, P. Sartori, E. Scharf, *Chem. Ber.* **1968**, *101*, 4214–4220.
[13] A. J. Edwards, G. R. Jones, *J. Chem. Soc. A* **1969**, *0*, 1467–1470.
[14] K. O. Christe, C. J. Schack, *Inorg. Chem.* **1970**, *9*, 2296–2299.
[15] J. Shamir, in *Structural Problems*, Springer, Berlin, Heidelberg, **1979**, pp. 141–210.
[16] I. C. Tornieporth-Oetting, T. M. Klapötke, *Heteroat. Chem.* **1993**, *4*, 543–552.
[17] L. B. Asprey, J. L. Margrave, M. E. Silverthorn, *J. Am. Chem. Soc.* **1961**, *83*, 2955–2956.
[18] J. Shamir, *Isr. J. Chem.* **1978**, *17*, 37–47.
[19] B. Scheibe, S. I. Ivlev, A. J. Karttunen, F. Kraus, *Eur. J. Inorg. Chem.* **2020**, *2020*, 1319–1324.
[20] P. Pröhm, J. R. Schmid, K. Sonnenberg, P. Voßnacker, S. Steinhauer, C. J. Schattenberg, R. Müller, M. Kaupp, S. Riedel, *Angew. Chem. Int. Ed.* **2020**, *59*, 16002–16006; *Angew. Chem.* **2020**, *132*, 16136–16140.
[21] S. I. Ivlev, A. J. Karttunen, M. R. Buchner, M. Conrad, F. Kraus, *Angew. Chem. Int. Ed.* **2018**, *57*, 14640–14644; *Angew. Chem.* **2018**, *130*, 14850.
[22] M. Y. Antipin, A. M. Ellern, V. F. Sukhoverkhov, Y. T. Struchkov, Y. A. Buslaev, *Russ. J. Inorg. Chem.* **1988**, *33*, 171–173.
[23] A. M. Ellern, M. Y. Antipin, A. V. Sharabarin, Y. T. Struchkov, *Russ. J. Inorg. Chem.* **1991**, *36*, 1278–1280.
[24] R. Bougon, W. V. Cicha, M. Lance, L. Meublat, M. Nierlich, J. Vigner, *Inorg. Chem.* **1991**, *30*, 102–109.
[25] A. M. Ellern, M. Y. Antipin, A. V. Sharabarin, Y. T. Struchkov, *Russ. J. Inorg. Chem.* **1992**, *37*, 46–47.
[26] A. M. Ellern, M. N. Sinitsyn, M. Y. Antipin, A. V. Sharabarin, Y. T. Struchkov, *Koord. Khim.* **1991**, *17*, 1686–1688.
[27] O. Ruff, E. Ascher, J. Fischer, F. Laass, *Z. Anorg. Allg. Chem.* **1928**, *176*, 258–270.
[28] H. Schmitz, H. J. Schumacher, *Z. Naturforsch. A* **1947**, *2*, 359–362.
[29] C. J. Schack, R. D. Wilson, *Synth. React. Inorg. Met.-Org. Chem.* **1973**, *3*, 393–396.
[30] C. J. Schack, R. D. Wilson, D. D. Desmarteau, in *Inorganic Syntheses* (Ed.: J. M. Shreeve), John Wiley & Sons, Inc., Hoboken, NJ, USA, **1986**, pp. 1–3.
[31] G. Natta, P. Corradini, *J. Polym. Sci.* **1959**, *39*, 29–46.
[32] C. De Rosa, F. Auriemma, *Crystals and Crystallinity in Polymers: Diffraction Analysis of Ordered and Disordered Crystals*, Wiley, Hoboken, New Jersey, **2013**.
[33] V. Kopský, D. B. Litvin (Eds.), *International Tables for Crystallography. Vol. E: Subperiodic Groups*, Wiley, Chichester, **2010**.
[34] U. Müller, *Acta Crystallogr., Sect. B: Struct. Crystallogr. Cryst. Chem.* **2017**, *73*, 443–452.
[35] O. Graudejus, A. P. Wilkinson, L. C. Chacón, N. Bartlett, *Inorg. Chem.* **2000**, *39*, 2794–2800.
[36] W. P. Davey, *Phys. Rev.* **1923**, *21*, 143–161.
[37] J. H. Burns, *Acta Crystallogr.* **1962**, *15*, 1098–1101.
[38] G. Lucier, J. Muenzenberg, W. J. Casteel, N. Bartlett, *Inorg. Chem.* **1995**, *34*, 2692–2698.
[39] G. Tavčar, E. Goreshnik, *J. Fluorine Chem.* **2016**, *189*, 33–38.
[40] U. Engelmann, B. G. Müller, *Z. Anorg. Allg. Chem.* **1991**, *598*, 103–110.
[41] J. P. Perdew, K. Burke, M. Ernzerhof, *Phys. Rev. Lett.* **1996**, *77*, 3865–3868.
[42] C. Adamo, V. Barone, *J. Chem. Phys.* **1999**, *110*, 6158–6170.
[43] K. O. Christe, X. Zhang, J. A. Sheehy, R. Bau, *J. Am. Chem. Soc.* **2001**, *123*, 6338–6348.
[44] *TURBOMOLE V7.2.1*, a Development of University of Karlsruhe and Forschungszentrum Karlsruhe GmbH, **1989**–**2007**, TURBOMOLE GmbH, since 2007, **2017**.
[45] F. Weigend, R. Ahlrichs, *Phys. Chem. Chem. Phys.* **2005**, *7*, 3297–3305.
[46] A. E. Reed, R. B. Weinstock, F. Weinhold, *J. Chem. Phys.* **1985**, *83*, 735–746.
[47] K. S. Thanthiriwatte, M. Vasiliu, D. A. Dixon, K. O. Christe, *Inorg. Chem.* **2012**, *51*, 10966–10982.
[48] J. F. Lehmann, G. J. Schrobilgen, K. O. Christe, A. Kornath, R. J. Suontamo, *Inorg. Chem.* **2004**, *43*, 6905–6921.
[49] D. A. Dixon, D. J. Grant, K. O. Christe, K. A. Peterson, *Inorg. Chem.* **2008**, *47*, 5485–5494.
[50] R. J. Gillespie, R. S. Nyholm, *Q. Rev. Chem. Soc.* **1957**, *11*, 339–380.
[51] M. Rahm, K. O. Christe, *ChemPhysChem* **2013**, *14*, 3714–3725.
[52] A. Kumar, S. R. Gadre, N. Mohan, C. H. Suresh, *J. Phys. Chem. A* **2014**, *118*, 526–532.
[53] M. Rahm, *J. Chem. Theory Comput.* **2015**, *11*, 3617–3628.
[54] A. D. Becke, K. E. Edgecombe, *J. Chem. Phys.* **1990**, *92*, 5397–5403.
[55] A. Savin, R. Nesper, S. Wengert, T. F. Fässler, *Angew. Chem. Int. Ed. Engl.* **1997**, *36*, 1808–1832; *Angew. Chem.* **1997**, *109*, 1892.
[56] R. D. Shannon, *Acta Crystallogr., Sect.* **1976**, *32*, 751–767.
[57] J. B. Mann, T. L. Meek, L. C. Allen, *J. Am. Chem. Soc.* **2000**, *122*, 2780–2783.
[58] J. B. Mann, T. L. Meek, E. T. Knight, J. F. Capitani, L. C. Allen, *J. Am. Chem. Soc.* **2000**, *122*, 5132–5137.
[59] R. T. Sanderson, *Polar Covalence*, Academic Press, New York, **1983**.
[60] K. O. Christe, R. D. Wilson, C. J. Schack, *Inorg. Synth.* **1986**, *24*, 3–6.
[61] *APEX3*, Bruker AXS Inc., Madison, Wisconsin, USA, **2018**.
[62] *X-Area*, STOE & Cie GmbH, Darmstadt, Germany, **2018**.
[63] G. M. Sheldrick, *Acta Crystallogr., Sect. A* **2015**, *71*, 3–8.
[64] G. M. Sheldrick, *Acta Crystallogr., Sect. C* **2015**, *71*, 3–8.
[65] A. L. Spek, *PLATON - A Multipurpose Crystallographic Tool*, Utrecht University, Utrecht, The Netherlands, **2019**.
[66] A. L. Spek, *Acta Crystallogr., Sect. D* **2009**, *65*, 148–155.
[67] G. M. Sheldrick, *CELL_NOW*, Göttingen (Germany), **2008**.
[68] S. I. Ivlev, M. Conrad, F. Kraus, *Z. Kristallogr. - Cryst. Mater.* **2019**, *234*, 415–418.
[69] K. Brandenburg, H. Putz, *Diamond - Crystal and Molecular Structure Visualization*, Crystal Impact GbR, Bonn, **2019**.
[70] R. Dovesi, A. Erba, R. Orlando, C. M. Zicovich-Wilson, B. Civalleri, L. Maschio, M. Rérat, S. Casassa, J. Baima, S. Salustro, B. Kirtman, *Wiley Interdiscip. Rev. : Comput. Mol. Sci.* **2018**, e1360.
[71] R. Ahlrichs, M. Bär, M. Häser, H. Horn, C. Kölmel, *Chem. Phys. Lett.* **1989**, *162*, 165–169.
[72] K. Eichkorn, O. Treutler, H. Öhm, M. Häser, R. Ahlrichs, *Chem. Phys. Lett.* **1995**, *240*, 283–290.
[73] F. Weigend, *Phys. Chem. Chem. Phys.* **2006**, *8*, 1057–1065.
[74] T. Lu, F. Chen, *J. Comput. Chem.* **2012**, *33*, 580–592.
[75] K. Momma, F. Izumi, *J. Appl. Crystallogr.* **2008**, *41*, 653–658.
[76] K. Momma, F. Izumi, *J. Appl. Crystallogr.* **2011**, *44*, 1272–1276.

Received: September 8, 2020